Binding and Hydrolysis of Nucleotides in the Chaperonin Catalytic Cycle: Implications for the Mechanism of Assisted Protein Folding†

Graham S. Jackson,*,‡ Rosemary A. Staniforth,‡ David J. Halsall,‡ Tony Atkinson,§ J. John Holbrook,‡ Anthony R. Clarke,‡ and Steven G. Burston‡

Molecular Recognition Centre and Department of Biochemistry, University of Bristol School of Medical Sciences, University Walk, Bristol BS8 1TD, U.K., and Microbial Technology Laboratory, Public Health Laboratory Service, Centre for Applied Microbiology and Research, Salisbury, Wiltshire SP4 0JG, U.K.

Received August 24, 1992; Revised Manuscript Received December 15, 1992

ABSTRACT: Cpn60 was labeled with pyrene maleimide in order to follow structural rearrangements in the protein triggered by the binding of nucleotides and cpn10. The conjugate binds ATP, AMP-PNP, and ADP(P_i) with pyrene fluorescence enhancements of 60%, 60%, and 15%, respectively. In each case, binding is cooperative with half-saturation ($K_{1/2}$) occurring at 10 μM, 290 μM, and 2500 μM and Hill constants (n_H) of 4, 3, and 3, respectively. Inclusion of the co-protein, cpn10, tightens the binding of ATP, AMP-PNP, and ADP(P_i) to give $K_{1/2}$ values of 6 μM, 100 μM, and <0.07 μM, respectively, and cooperativity is increased. Titration of the cpn60/ADP (14-mer) complex with cpn10 (7-mer) gives a stoichiometry of 14:7 with respect to subunits, confirming the molecular asymmetry shown by electron microscopy. Transient kinetics demonstrate that ATP initially forms a weak collision complex with cpn60 (K_d = 4 mM) which isomerizes to the strongly binding state at a rate of 180 s^{-1}. We suggest that the slow structural rearrangement driven by ATP binding is the same event which lowers the affinity of the chaperonin for protein substrates; a suggestion reinforced by the loss of AMP-PNP binding affinity in the presence of an unstructured polypeptide. As such, this rearrangement of cpn60 is analogous to a force-generating step in energy transduction. Measurements of ATP hydrolysis (pH 7.5, 25 °C) show that it is slow (0.04 s^{-1}) compared both with the structural rearrangement and with the dissociation of products. This defines the steady-state complex as cpn60/ATP, a form of the chaperonin which binds substrate proteins weakly. The rate of hydrolysis of ATP is stimulated 20-fold upon binding unfolded lactate dehydrogenase, and the yield of folded enzyme is increased even in the absence of cpn10. Addition of this co-protein inhibits hydrolysis on only half of the sites in cpn60 and leads to a faster release of folded LDH. A mechanism for the action of chaperonins is proposed which depends upon cpn60 being cycled between states which have, alternately, low and high affinity for unfolded proteins. This cycle is driven by the binding and hydrolysis of ATP.

The most widely demonstrated cellular function of chaperonins is to facilitate the folding and assembly of protein chains into biologically active structures [for reviews, see Gatenby and Ellis (1990), Ellis and van der Vies (1991), Lorimer (1992), Rothman (1989), Zeilstra-Ryalls et al. (1991), and Gething and Sambrook (1992)]. This activity can be mimicked in vitro by unfolding proteins in denaturants and allowing them to renature in the presence of chaperonins. For proteins which refold with poor efficiency in vitro, chaperonins have been shown to improve the yield of the native form (Tandon & Horowitz, 1986; Goloubinoff et al., 1989; Martin et al., 1991; Buchner et al., 1991).

The chaperonin system has three components; the major protein cpn60 (GroEL), the co-protein cpn10 (GroES), and Mg–ATP. The cpn60 oligomer contains 14 subunits arranged in a double ring, each comprising seven identical subunits (Hohn et al., 1979; Hendrix, 1979; Ishii et al., 1992). The cpn10 co-protein contains seven identical subunits arranged in a single ring (Chandrasekhar et al., 1986). In the presence of Mg–ATP, cpn10 is seen under the electron microscope to associate with only one end of the cpn60 structure (Saibil et al., 1991). That is, the co-protein only makes contact with half of the subunits in the cpn60 oligomer. The subunit stoichiometry of 14 cpn60 to 7 cpn10 has been determined in functional assays of the chaperonins (Chandrasekhar et al., 1986; Martin et al., 1991).

An increase in folding efficiency for some protein substrates can be achieved by incubation of the denaturated protein with cpn60 alone (Badcoe et al., 1991; Brown et al., 1992; Schmidt & Buchner, 1992). Here, the rate of folding is markedly slower than in the spontaneous process, and the increased yield of the native state can be explained by the suppression of aggregation of unfolded protein chains (Buchner et al., 1991). Thus for the simplest, irreversible case, the rate of folding (V_f) can be represented:

$$V_f = [U]k_f$$

where [U] is the concentration of the unfolded form before it undergoes a unimolecular rate-determining step in its conversion to the native state, the rate constant for this step being k_f. The rate of irreversible aggregation (V_a), given that it is due to a bimolecular collision of unfolded chains (with second order rate constant k_a), becomes:

$$V_a = [U]^2k_a$$

In protein folding, these processes often compete, the partition ratio (p) between the processes of folding and aggregation can be described:

$$p = V_f/V_a = k_f/([U]k_a)$$

Thus, if by binding the unfolded form the chaperonin reduces

† This work was supported by a grant from The Wellcome Trust.
* Author to whom correspondence should be addressed.
‡ University of Bristol School of Medical Sciences.
§ Center for Applied Microbiology and Research.

0006-2960/93/0432-2554$04.00/0

its free concentration [U], the ratio (p) will increase and folding is favored over aggregation. The penalty paid for this "passive chaperoning" is a decrease in the folding rate (V_f) owing to a reduction in the concentration of species U which is available to undergo folding.

For many proteins, however, the addition of Mg–ATP is necessary to release them from cpn60 (Martin et al., 1991; Buchner et al., 1991) and for others both Mg–ATP and the co-protein, cpn10, are required (Goloubinoff et al., 1989; Martin et al., 1991). In these latter cases, large increases in folding efficiency are observed without markedly slowing the rate of folding over that measured in the absence of chaperonins. This contradicts the simple passive mechanism described above and suggests that the energy derived from ATP hydrolysis is being directed into the folding process.

In determining how this transduction of energy is achieved, it is important to understand the interactions between cpn60 and its protein and nucleotide ligands, and to establish the basic cycle of ATP hydrolysis in these complexes. In this paper, we describe a fluorescent signal on cpn60 which reports the interconversion between two, hitherto proposed structural states (Badcoe et al., 1991; Baneyx & Gatenby, 1992) and use it to explore the formation of complexes between cpn60, nucleotides, and the co-protein cpn10. We use steady-state and transient kinetics to identify and measure the rate-limiting step in the binding–hydrolysis–release cycle of ATP. We also quantify the effect of unfolded protein on the rate and extent of ATP hydrolysis in both cpn60 and the cpn60/cpn10 complex. The findings both define the predominant chaperonin/nucleotide complexes in the steady-state and suggest a mechanism for the action of chaperonins in protein folding.

MATERIALS AND METHODS

Preparation of Proteins. Escherichia coli cpn60 and cpn10 were coexpressed in *E. coli* MC1061 cells from the pND5 plasmid (Jenkins et al., 1986) and prepared by a modification of the procedure described by Chandrasekhar et al. (1986). Cultures were grown for 18 h at 37 °C, followed by a 1-h heat shock at 42 °C and a final 1 h of growth at 37 °C. Cells were disrupted by sonication, and the soluble fraction precipitated in 70% saturation of ammonium sulfate. Precipitated protein was resuspended in 50 mM triethanolamine hydrochloride (TEA), pH 7.5, and dialyzed against 200 volumes of this buffer overnight. Soluble material was loaded onto a Q-Sepharose ion-exchange column and fractions eluted by a 0–0.6 M NaCl gradient. Cpn10 eluted at 0.2 M NaCl and was purified to homogeneity by gel filtration using a CL-6B Sepharose column and a further ion-exchange step using Q-Sepharose. Cpn60 elutes at 0.4 M NaCl and, after dialysis, was subjected to further Q-Sepharose ion-exchange chromatography to yield pure protein. After purification, both proteins were stored as a precipitate in 70% saturated ammonium sulfate. Prior to use, both proteins were dialyzed against 300–500 volumes of 50 mM TEA, pH 7.5, 50 mM KCl, and 20 mM $MgCl_2$ containing 0.5 mg/mL acid-washed charcoal for 10–18 h. The dialyzed proteins were stored at 4 °C and used within 36 h. The concentration of cpn60 was determined as described previously (Badcoe et al., 1991). The concentration of cpn10 was estimated assuming an absorption at 280 nm of 0.12 for a 1 mg/mL solution, calculated from the aromatic content of the constituent amino acids in its gene-derived sequence (Jenkins et al., 1986).

Standard Buffer Conditions. The standard buffer for all of the experiments presented in this paper, except where stated, is 50 mM triethanolamine hydrochloride (TEA), pH 7.5, 50 mM KCl, and 20 mM $MgCl_2$ and is hereafter referred to as the standard buffer. All experiments were performed at 25 °C.

Assay of the Phosphate Content in Cpn60. Owing to a recent report that cpn60 is phosphorylated upon heat-shock in *E. coli* cells (Sherman & Goldberg, 1992), we assayed the purified protein for its phosphate content using NaOH hyrolysis and a subsequent colorimetric phosphate assay using ammonium molybdate (Ames, 1966). Fewer than one molecule in 100 carried a phosphate group. The cpn60 protein was also tested for its ability to catalyze autophosphorylation; 100 μL of 50 μM protein (subunits) was incubated with 1 mM Mg–ATP containing 1 μCi of [γ-^{32}P]Mg–ATP. The reaction was carried out at 25 °C for 120 min. After this period, the protein was precipitated by the addition of 10 μL of 100% w/v trichloroacetic acid. The precipitate was centrifuged, and the pellet was washed three times with 1-mL aliquots of 10% trichloroacetic acid before being dissolved in 1 mL of 6 M guanidinium chloride (GuHCl). The sample was then tested for radioactivity by Cerenkov counting in a Packard Tri-Carb scintillation analyzer. There was no statistically significant difference in counts between this sample and an identical preparation incubated with cold Mg–ATP. We conclude that in these conditions cpn60 does not phosphorylate itself to produce a stable conjugate in the presence of Mg–ATP.

Labeling with Pyrene Maleimide. One milliliter of 300 μM cpn60 (subunits) in standard buffer was mixed with 47 μL of 0.5 mM pyrene maleimide dissolved in ethanol. The reaction was allowed to go to completion (2 h), and the resultant dye–protein conjugate was precipitated by the addition of ammonium sulfate (70% saturation). After centrifugation at 13 000 rpm for 12 min, the pellet was resuspended in 500 μL of the standard buffer (see above) and dialyzed overnight against the same buffer containing 0.5 mg/mL acid-washed charcoal. Spectrophotometric analysis showed that more than 90% of the label had been incorporated into the protein in these conditions. The concentration of incorporated dye was estimated by assuming an extinction coefficient for cysteinyl-pyrene of 22 000 at a wavelength of 340 nm (Kouyami & Mihashi, 1981). The labeling ratio was one pyrene group per 15 subunits of cpn60, that is approximately one label per 14-mer cpn60 complex (see Figure 1).

Assay for Mg–ATP Hydrolysis by Cpn60. Mg–ATPase activity was assayed by a modification of the methods described by Zimmerman (1963) and Godchaux and Zimmerman (1979). The protein was mixed with 1 mM Mg–ATP containing 500 nCi of [γ-^{32}P]ATP in the standard buffer (see above). Aliquots were withdrawn at given time intervals and mixed with four volumes of 0.5 M EDTA (pH 4.5) containing 20 mg/mL acid-washed charcoal, thus quenching enzymatic activity. The suspension was then centrifuged, and the supernatant containing the hydrolyzed phosphate groups was subjected to Cerenkov radiation counting. All nucleotide and protein material was adsorbed onto the charcoal so that any counts associated with unhydrolyzed Mg–ATP were removed. The background activity derived from spontaneously hydrolyzed phosphate in the original radioactive Mg–ATP preparation was subtracted from all results. The count rates were related to the amount of Mg–ATP hydrolyzed by measuring the radioactivity of an identical assay sample not treated with charcoal. This method measures the total product formed, whether it is free in solution or bound to the enzyme.

Fluorescence Measurements. All equilibrium experiments were performed on a Perkin-Elmer LS50B spectrofluorometer. In order to measure fluorescence changes in the dye–protein

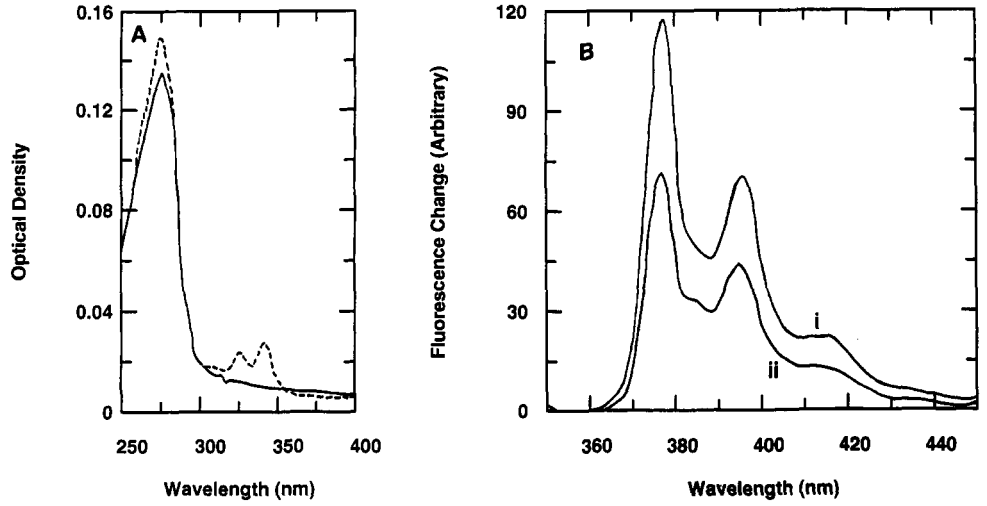

FIGURE 1: Optical properties of pyrenyl-cpn60. Plot A shows the absorption spectra of cpn60 (—) and the cpn60–pyrene conjugate (- - -) while plot (B) shows the fluorescence emission spectrum, both in the presence of 1 mM ATP (i) and in the absence of ATP (ii). Peak emission is at 375 nm with a 60% enhancement in pyrene fluorescence in the presence of ATP. The concentration of cpn60 oligomer in each case was 0.8 μM and the buffer conditions were 50 mM TEA, pH 7.5, 50 mM KCl, and 20 mM $MgCl_2$ (the standard experimental buffer).

conjugate upon ligand binding, the pyrenyl label was excited at 340 nm and fluorescence emission was monitored at 375 nm. The excitation and emission slit widths were set at 5 nm. All experiments were repeated three times, and the figures show representative data sets. Rapid reactions were observed using a Hi-Tech (Salisbury, Wiltshire, U.K.) stopped-flow SF51 spectrofluorometer. The sample was excited with monochromated light at a wavelength of 325 nm from a mercury–xenon lamp. Emitted light was selected using a filter cutting off light at wavelengths lower than 360 nm. Each recorded transient was an average of five individual reactions.

Refolding of L-*Lactate Dehydrogenase (LDH).* Lactate dehydrogenase from *Bacillus stearothermophilus* was prepared as described previously (Clarke et al., 1985) and denatured in 4 M GuHCl containing 2 mM dithiothreitol (DTT). The enzyme was refolded in a solution of 0.2 mM NADH and 10 mM pyruvate in the standard buffer (Badcoe et al., 1991). The regain of LDH enzymatic activity was detected by monitoring the decrease in NADH absorption at 340 nm in order to measure the effect of the chaperonins and ATP hydrolysis on this process. The reaction was carried out with these components premixed in the assay cuvette.

Fitting of Experimental Data. Experimental data was fitted using the nonlinear least-squares method of Marquardt (1963) using the graphics software Grafit v2.0. (Leatherbarrow, 1990).

RESULTS

Figure 1 shows the absorption and fluorescence emission spectra of cpn60 labeled with one pyrene group per oligomer. There was a 60% enhancement of the fluorescence emission intensity upon the addition of Mg–ATP to the protein which was not accompanied by a measurable shift in the wavelength of the emission maximum. The change in protein fluorescence was not caused by autophosphorylation (see Materials and Methods). This signal was subsequently used for following the binding of nucleotides and cpn10 to the protein. In order to determine whether labeling had altered the functional integrity of the protein, we compared the ability of labeled and unlabeled cpn60 to bind and hydrolyze ATP. The results demonstrated that the steady-state rate of Mg–ATP hydrolysis was not changed measurably (±5%) by the attachment of the dye (data not shown). The turnover rate of Mg–ATP was 0.038 (±0.003) mol per subunit per second. The ability of cpn60 to bind cpn10 was also unaffected (see later results).

Binding and Hydrolysis of Mg–ATP by Cpn60 and the Effect of Cpn10. The fluorescence enhancement on addition of Mg–ATP was used to obtain a binding curve in the presence and absence of the co-protein, cpn10 (Figure 2A). The increase in fluorescence on addition of Mg–ATP was instant on the time scale of this experiment (within 2 s) yet the steady-state hydrolysis rate was slow (see below, Figure 9A). This showed that the formation of the cpn60/Mg–ATP complex with enhanced fluorescence was rapid compared to hydrolysis and that the data in Figure 2A represent real binding curves. This point is also demonstrated in the experiment shown in Figure 3 (i) where cpn60 was mixed with about 50 site-equivalents of Mg–ATP and the fluorescence was measured over a long time course. There was a rapid formation of the high-fluorescence cpn60/Mg–ATP state which returned slowly to the low fluorescence apo-cpn60 state only after exhaustion of the substrate. When this experiment was repeated in the presence of cpn10, the high fluorescence state persisted for longer than 1000 s, showing that even the depletion of Mg–ATP does not lead to dissociation of the high fluorescence protein/nucleotide complex (Figure 3 (ii)). This can be explained by two effects: (1) the slow hydrolysis of ATP (see Figure 9A) and (2) the high stability of the cpn60/cpn10/ADP complex (see Figure 5B).

In the absence of cpn10, Mg–ATP binding was shown to be cooperative with a Hill constant of 4(±0.5) and a $K_{1/2}$ of 10 μM. In the presence of cpn10, cooperativity was increased; the Hill constant rose to 6(±0.5) and the $K_{1/2}$ was reduced to 6 μM. We define $K_{1/2}$ here as the nucleotide concentration required for half the fluorescence change.

Binding of a Nonhydrolyzable ATP Analogue to Cpn60. Given that the structural change reported by extrinsic fluorescence appears to be driven by nucleotide binding rather than hydrolysis, then the same response should be seen when pyrenyl-cpn60 is titrated with adenylyl imidodiphosphate (AMP-PNP). This analogue of ATP cannot be hydrolyzed in the active site but is able to displace protein substrates from cpn60 (Badcoe et al., 1991). The results in Figure 2B show this prediction to be true. Mg–AMP-PNP bound cooperatively to cpn60 and stimulated the same fluorescence enhancement as Mg–ATP. The analogue bound 30 times more weakly

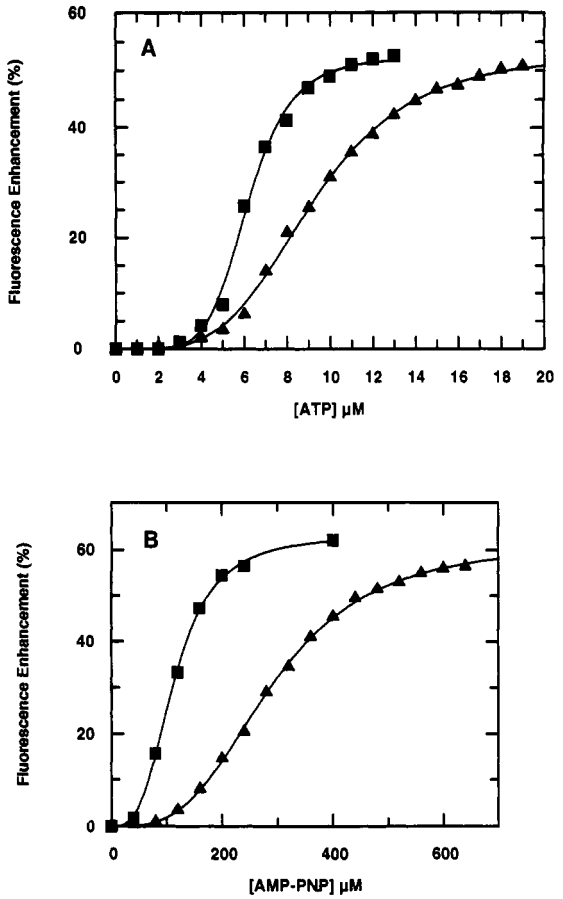

FIGURE 2: Equilibrium binding of ATP and AMP-PNP. Plot A shows the fluorescence enhancement at 375 nm as ATP was titrated into 54 nM cpn60 oligomer in the absence (▲) and presence (■) of 150 nM cpn10 oligomer in the standard buffer. The solid line in each case shows the optimal fit of the data to the Hill equation with parameters $n_H = 4$, $K_{1/2} = 10$ μM in the absence and $n_H = 6$, $K_{1/2} = 6$ μM in the presence of cpn10. The results in plot B show the binding of Mg–AMP-PNP to 54 nM cpn60 oligomer in the absence (▲) and presence (■) of 150 nM cpn10 oligomer in conditions identical to those in (A). The solid line shows the optimal fit of the data to the Hill equation with parameters $n_H = 3$, $K_{1/2} = 290$ μM in the absence and $n_H = 3.5$, $K_{1/2} = 110$ μM in the presence of cpn10.

($K_{1/2}$ = 290(±20) μM, Hill constant = 3(±0.5)), but, as in the case of Mg–ATP binding, its interaction was tightened in the presence of cpn10 ($K_{1/2}$ = 110(±10) μM, Hill constant = 3.5(±0.5)).

Stopped-Flow Analysis of the Mg–ATP-Induced Conformational Rearrangement of Cpn60. When a 5-fold excess of Mg–ATP was rapidly mixed with labeled cpn60 in equal volumes in a stopped-flow fluorometer, the pyrene fluorescence was seen to rise as a single-exponential process. As the nucleotide concentration was increased, the observed rate constant for this process rose to a maximum. A plot of the observed rate constant (k_{obs}) against Mg–ATP concentration is shown in Figure 4. This response is saturable showing that the rate of fluorescence change is not limited by diffusion but by some slower protein isomerization step following formation of the collision complex. The reaction on a single subunit of cpn60 is most simply described as:

$$\text{cpn60} + \text{Mg–ATP} \overset{K_1}{\rightleftharpoons} \text{cpn60/Mg–ATP} \overset{k_2}{\underset{k_{-2}}{\rightleftharpoons}} {}^*\text{cpn60/Mg–ATP}$$

where the asterisk denotes the high fluorescence state. The

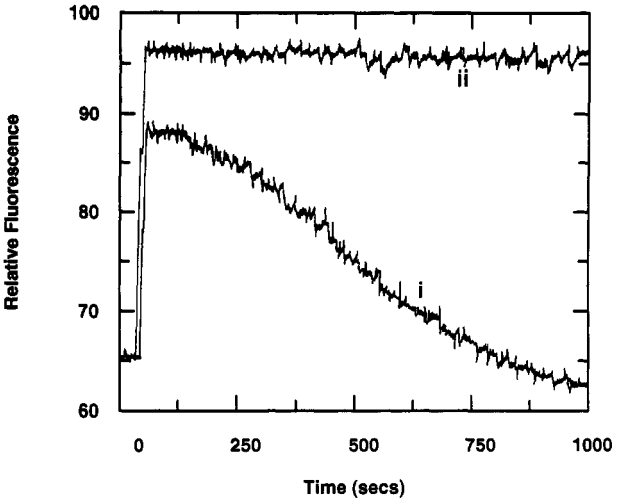

FIGURE 3: Time course of fluorescence response during ATP hydrolysis. Trace i shows the fluorescence response at 375 nm of the pyrene group on addition of 40 μM ATP to 54 nM cpn60 oligomer in the standard buffer. Trace ii shows a similar addition, but to the buffer containing 54 nM cpn60 and 500 nM cpn10 oligomer.

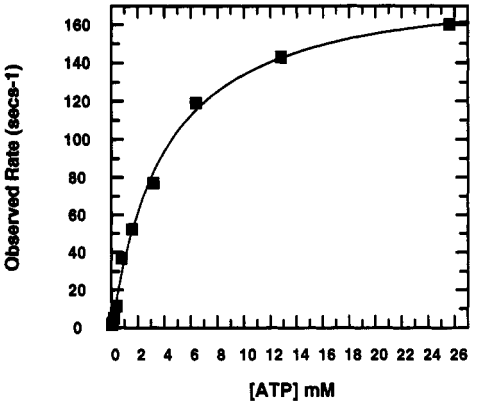

FIGURE 4: Stopped-flow analysis of ATP binding. The plot shows the observed first-order rate constants (k_{obs}) measured from the rapid kinetics of formation of the cpn60/ATP complex. The fluorescence change was monitored when pyrenyl-cpn60 was rapidly mixed in a stopped-flow fluorometer with increasing concentrations of ATP in the standard buffer. The concentration of cpn60 after mixing was 10 μM subunits. The solid line shows the best fit of the data to the hyperbolic relationship described in Results. The maximum rate at saturating concentrations of Mg–ATP (k_2) is 180 s^{-1} and the ATP concentration at which the rate is half-maximal (K_1) is 4 mM. The reverse conformational change (k_{-2}) represented by the y-axis intercept is negligible.

equation describing the rapid kinetics for such a system is:

$$k_{obs} = k_2 \frac{[\text{Mg–ATP}]}{K_1 + [\text{Mg–ATP}]} + k_{-2}$$

The signal, therefore, did not arise from the pyrene group being directly sensitive to proximal collision binding of the ligand but reported a slower rearrangement of the subunits which was triggered by this initial event. At saturating ATP concentrations this rearrangement (k_2) occurred at 180(±20) s^{-1}. The concentration of ATP at which this structural event proceeded at half its maximal rate was 4(±1) mM, a concentration some 400 times higher than that required for half-saturation of the protein at equilibrium (10 μM). Thus, the weak interaction of cpn60 with Mg–ATP (described by the equilibrium constant, K_1) drives a conversion of the protein to a new structure which binds the nucleotide at least 400 times more tightly.

Association of Cpn60 and Mg–ADP. Figure 5A shows that Mg–ADP bound only weakly to cpn60 ($K_{1/2}$ = 2.3(±0.2)

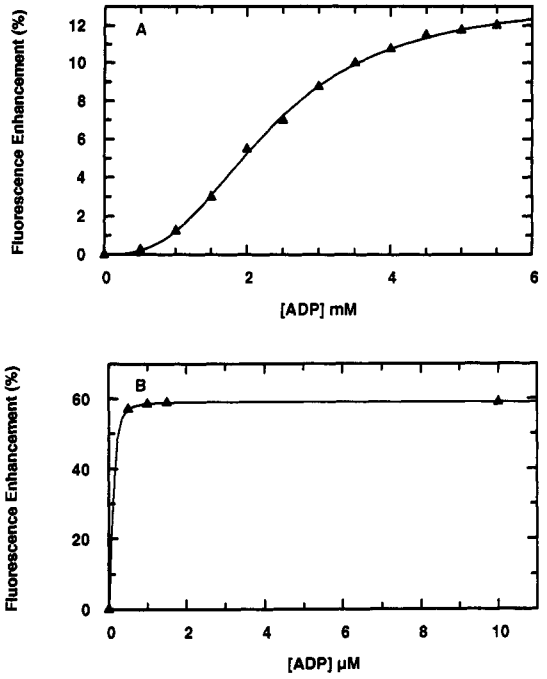

FIGURE 5: Equilibrium binding of ADP. Plot A shows the result of titrating ADP into 54 nM cpn60 oligomer in the standard buffer and measuring the fluorescence enhancement at 375 nm. The line through the data represents the optimal fit to the Hill equation, giving the values $n_H = 3$ and $K_{1/2} = 2.3$ mM. The experiment was repeated in the presence of 140 nM cpn10 and is shown in plot B. This illustrates the large increase in affinity of cpn60 for Mg–ADP in the presence of 140 nM cpn10 ($K_{1/2} < 70$ nM). In this case, the solid line does not represent a fit of the data but is included to emphasize the tight binding of ADP to the cpn60/cpn10 complex.

mM) and caused a fluorescence enhancement of a much smaller amplitude (10%) than did either Mg–ATP or Mg–AMP-PNP. However, it remained cooperative with a Hill coefficient of approximately 3. The addition of 10 mM sodium orthophosphate to cpn60 elicited no fluorescence response in the protein conjugate. Furthermore, when the protein was titrated with Mg–ADP in the presence of 10 mM sodium orthophosphate, the binding curve was unchanged (results not shown). We conclude that there is no stable ADP·P_i state and that phosphate binding either is extremely weak or causes no conformational change in the protein. The inclusion of cpn10 in the titration increased the Mg–ADP binding affinity massively and gave a greater fluorescence change (Figure 5B). At only 1 μM Mg–ADP (with 0.75 μM cpn60 sites), there was a fluorescence enhancement of 50% which showed no appreciable change as the nucleotide concentration was increased. The fluorescence enhancement was at least 90% complete at 1 μM Mg–ADP. Assuming only half of the sites (giving a concentration of 0.375 μM) bind Mg–ADP tightly in the presence of cpn10 (see next section), then:

$$K = \frac{[s]}{\alpha} - [s] = \frac{(1 - 0.375)}{0.9} - (1 - 0.375) = 0.069\ \mu M$$

where α is the fractional saturation of sites and [s] is the concentration of free Mg–ADP. We infer that the binding sites are half-saturated at free Mg–ADP concentrations of, at most, 70 nM. Thus, cpn10 must increase the affinity of cpn60 for Mg–ADP by at least 33 000-fold. The cpn60/Mg–ADP/cpn10 complex formed extremely slowly, even in saturating concentrations of Mg–ADP (see Figure 6). At saturating concentrations of Mg–ADP, the apparent first-order rate constant was about 0.014 s^{-1}, thus when the Mg–ADP concentration is low the components must be incubated

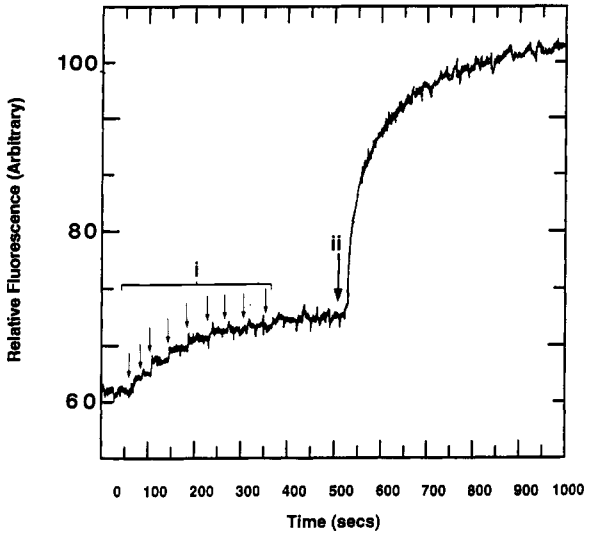

FIGURE 6: Slow formation of the cpn60/ADP/cpn10 complex. (i) Cpn60 oligomer (54 nm) was saturated with successive aliquots of 0.5 mM ADP in the standard buffer followed by the addition of 140 nM cpn10 oligomer at (ii). The increase in fluorescence at 375 nm illustrates the slow formation of the cpn60/Mg–ADP/cpn10 complex.

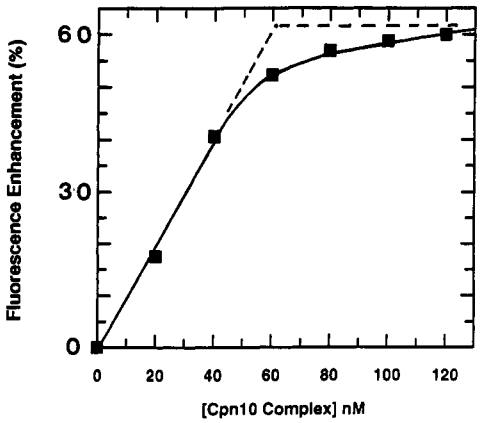

FIGURE 7: Stoichiometry and affinity of cpn10 binding to cpn60/ADP. Aliquots of cpn10 oligomer were titrated into 54 nM cpn60 oligomer in 50 mM TEA, pH 7.5, 50 mM KCl, 25 mM $MgCl_2$, 25 mM ADP, and the fluorescence enhancement at 375 nm was monitored. Superimposed is the nonlinear fit of the data to the following tight binding equation $F = (((L + E_0 + K_d) - ((L + E_0 + K_d)^2 - 4.E_0L)^{-2}/2E_0)(F_{min} - F_{max})) + F_{max}$, where L is the concentration of cpn10, E_0 is the cpn60 concentration, K_d is the dissociation constant of the cpn10, F is the observed fluorescence intensity, and F_{min} and F_{max} are the minimum and maximum intensities, respectively. The dashed lines emphasize the 1:1 stoichiometry in the complex.

for long periods in order to reach equilibrium. In the experiment shown in Figure 7, the components when incubated for 20 h in order to reach equilibrium. The rate of 0.014 s^{-1} was achieved at a cpn10 (7-mer) concentration of 140 nM, the apparent collision rate was therefore 1×10^5 M^{-1} s^{-1}.

Stoichiometry of Cpn60 to Cpn10 in the Ternary Complex Formed with Mg–ADP. The fact that the fluorescence of the cpn60/Mg–ADP complex was different from that seen in cpn60/Mg–ADP/cpn10 provided a simple and direct way of determining the stoichiometry of the protein–co-protein interaction. Figure 7 shows the result of an experiment in which cpn60 (0.75 μM subunits/0.054 μM 14-mer) was firstly saturated with Mg–ADP and then titrated with cpn10. The data, when analyzed according to the equation described in the legend, showed that 0.056(±0.005) μM cpn10 (7-mer) was bound to the complex, thus indicating that one cpn60 oligomer associates with one cpn10 oligomer. The dissociation

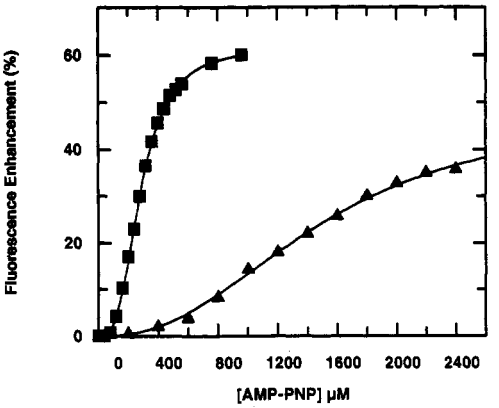

FIGURE 8: AMP-PNP binding to cpn60 in the presence of a peptide. Aliquots of AMP-PNP were added to 54 nM cpn60 oligomer (■) in the standard buffer and the fluorescence enhancement at 375 nm was recorded. The experiment was repeated with the addition of AMP-PNP to cpn60 in the presence of 100 μM 26-mer synthetic peptide (FKPPKYHPDVPYVKRVKTWRMHLFTG) (▲).

constant, K_d, for the protein–protein interaction was extremely small, 0.5–3 nM in terms of oligomers.

Binding of Nucleotide in the Presence of an Unstructured Peptide. The hypothesis that binding of ATP or analogous provides the energy for a protein conformational change from the apo-cpn60 state, which has a high affinity for nonnative proteins, to a cpn60/nucleotide complex with low affinity for protein (Badcoe et al., 1991; Baneyx & Gatenby, 1992), would predict a weaker association between Mg–AMP-PNP and a cpn60/peptide complex. Figure 8 shows binding curves resulting from the addition of Mg–AMP-PNP to a preequilibrated cpn60/peptide complex and to cpn60 alone. In the presence of a peptide (for the primary sequence see the legend to Figure 8), binding was weakened by a factor of 5, with a $K_{1/2}$ of 1.5(±0.2) mM and a Hill constant of 2(±1) as opposed to a $K_{1/2}$ of 290 μM and Hill constant of 3 for cpn60 alone.

Effect of Cpn10 on the Steady-State Rate of Mg–ATP Hydrolysis by Cpn60. The maximum steady-state rates of Mg–ATP hydrolysis by cpn60 are shown in Figure 9A. The result shows the catalytic rate for a cpn60 subunit in the absence of cpn10 to be 0.038 s^{-1} while in the presence of a 2-fold excess of the co-protein the rate is approximately halved to 0.018 s^{-1}. In these experiments, an increase in the concentration of Mg–ATP and/or cpn10 had no appreciable effect on the rates, showing that cpn60 was saturated with respect to both ligands [see also Gray and Fersht (1991)]. The lack of a rapid phase at the beginning of the reaction, with an amplitude corresponding to the concentration of subunits (260 μM), indicates that the release of the hydrolytic products is not limiting the steady-state reaction rate.

To determine the cpn60/cpn10 stoichiometry in the assay conditions used here, the steady-state rate of Mg–ATP hydrolysis by cpn60 was measured as a function of cpn10 in the assay (data not shown). The reaction mixtures contained 10 μM cpn60 subunits (0.71 μM 14-mer) and saturating Mg–ATP (1 mM). Eleven reactions were performed at increasing concentrations of cpn10 from 0 to 10 μM (subunits). There was a linear decline in the steady-state rate from 0.039 s^{-1} in the absence of cpn10 to 0.019 s^{-1} in the presence of 5 μM cpn10 subunits (0.71 μM 7-mer). Higher concentrations of co-protein had no further effect. These results demonstrate that the protein–protein interaction is tight and confirm that 1 mol of cpn10 7-mer is sufficient to saturate 1 mol of cpn60 14-mer so reducing the hydrolysis rate by half.

These observations imply that the halving of the steady-state ATPase rate is a result of cpn10 inhibiting the active

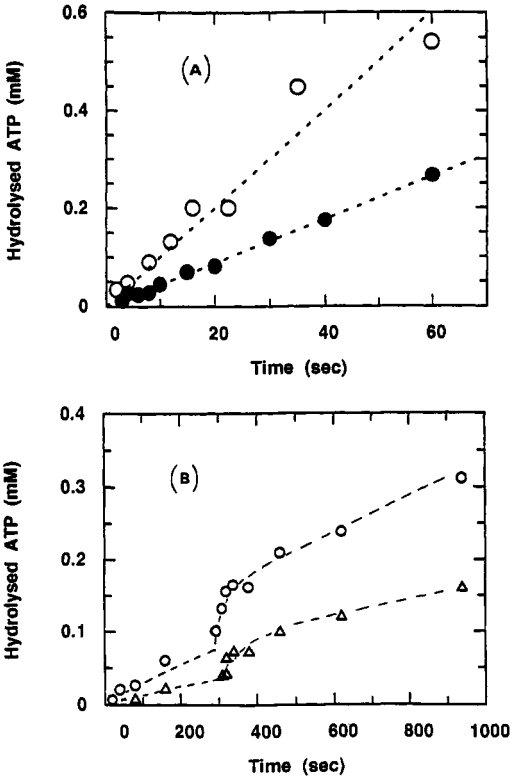

FIGURE 9: ATP hydrolysis and the effect of unfolded LDH. Steady-state reactions were set up using (A) 260 μM cpn60 subunits in 50 mM TEA, pH 7.5, 50 mM KCl, 20 mM $MgCl_2$, and 2 mM ATP (containing 500 nCi of [γ-^{32}P]ATP) in the presence (●) and absence (○) of 260 μM cpn10. Aliquots were withdrawn and the amount of ATP hydrolyzed was measured as described in Materials and Methods. The dashed lines are linear regressions and show rates of turnover of 0.038 s^{-1} per site in the absence of cpn10 and 0.018 s^{-1} per site in the presence of cpn10. Further steady-state reactions were set up in (B) using 7 μM cpn60 subunits in the presence (△) and absence (○) of 28 μM cpn10 subunits. After a 5-min reaction time, 2 μM denaturated LDH subunits was added and the subsequent burst of ATP hydrolysis was monitored.

sites of half of the subunits in the cpn60 14-mer. However, another possibility is that all of the subunits hydrolyze Mg–ATP at half the maximal rate. To distinguish between these possibilities the ATPase reaction was carried out under "single-turnover" conditions. Equal concentrations of Mg–ATP and cpn60 subunits (0.2 mM) were mixed and the amount of product was measured as the reaction progressed. Thus, each active site need go through only one hydrolytic cycle. The concentration of Mg–ATP was sufficient to saturate the cpn60 (see above). The result of this experiment (Figure 10) demonstrates that Mg–ATP is hydrolyzed in a single exponential process with an observed rate constant of 0.043 s^{-1}, the same as the maximum catalytic rate for hydrolysis in the steady state. Thus, it must be hydrolysis of Mg–ATP and not the release of products which limits the rate of the ATPase cycle. The predominant complex in the steady state is therefore cpn60/Mg–ATP.

When this "single-turnover" reaction is performed in the presence of excess cpn10 (see Figure 10), the reaction proceeds in two phases. Half the Mg–ATP is hydrolyzed at 0.042 s^{-1} and half considerably slower (0.004 s^{-1}). This demonstrates than cpn10 inhibits Mg–ATP hydrolysis on only one side of the cpn60 oligomer and that equilibrium of Mg–ATP between sites on each side of the complex is relatively slow.

Effect of Unfolded Protein on ATP Hydrolysis. The function of the chaperonin complexes is to couple the energy released by ATP hydrolysis to an enhancement of protein

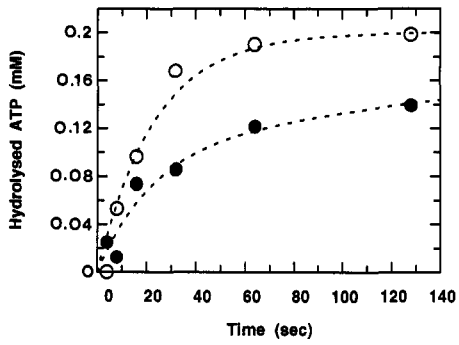

FIGURE 10: Single-turnover hydrolysis of ATP. Cpn60 subunits (200 μM) were mixed with 200 μM [γ-^{32}P]ATP in the absence (○) and presence (●) of 400 μM cpn10 subunits in the standard buffer. These conditions allowed a single turnover of the catalytic cycle to be studied. At given time intervals the reaction was quenched and the total ATP hydrolyzed was measured as described in Materials and Methods. The data points were fitted to a single exponential (k = 0.04 s^{-1}) for cpn60 alone and a double exponential (k_1 = 0.04 s^{-1} and k_2 = 0.004 s^{-1}) in the presence of cpn10. For the latter, the amplitudes of the fast and slow phases were 0.11 and 0.08 mM ATP, respectively.

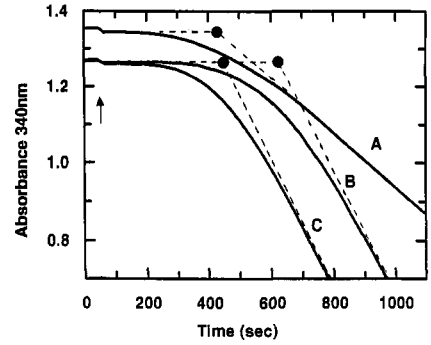

FIGURE 11: LDH refolding in the presence and absence of chaperonins. The refolding of LDH was monitored by measuring the conversion of NADH to NAD$^+$ by the change in absorbance at 340 nm (Badcoe et al., 1991). LDH unfolded in 4M quanidine hydrochloride was added to a 1-mL solution of the standard buffer containing 3.5 mM ATP, 5 mM pyruvate, 0.02 mM NADH, and 2 mM DTT. This refolding reaction was carried out in the absence of chaperonins (a) and in the presence of 0.4 μM cpn60 oligomers (b) and 0.4 μM cpn60/1 μM cpn10 oligomers (c). The arrow marks the points of addition of the unfolded LDH, and the bracket represents the lagtime for the refolding process. For clarity, the refolding curve for LDH in the absence of chaperonins is offset on the y-axis by 0.1 absorption unit.

folding efficiency. In the absence of an unfolded protein substrate, it is predictable that the ATPase activity of chaperonins will be low to prevent wastage of ATP. Given the ability of cpn10 to inhibit hydrolysis in the absence of a protein substrate, we wished to see whether this was true when the complex was challenged with a 4-fold excess of an unfolded protein. Figure 9B shows the progress of Mg–ATP hydrolysis of cpn60 in the presence and absence of cpn10. At a given time in the steady-state reaction, unfolded lactate dehydrogenase was introduced. In the absence of cpn10 the ATPase rate was immediately increased by a factor of at least 20 and returned to its original rate after 20–30 s. During this period, approximately 200 molecules of ATP were hydrolyzed per cpn60 oligomer. In the presence of cpn10, all rates were approximately halved and only 80 molecules of ATP were hydrolyzed. It is probable, therefore, that when the ATPase reaction is coupled to protein folding, the co-protein remains part of the complex and continues to block ATP turnover either by inhibiting hydrolysis (Figure 10) or by preventing ADP release (Figure 5B).

Effect of Chaperonins on the Efficiency of LDH Folding. The influence of chaperonins on the efficiency and rate of LDH refolding is demonstrated in Figure 11. The enzyme was refolded from the denatured state in an assay buffer, such that the slope of the curve at any point is proportional to the concentration of refolded LDH. The experiment was carried out in the absence of chaperonins, in the presence of cpn60 and Mg–ATP, and in the presence of cpn60, cpn10, and Mg–ATP. Cpn60, both with and without the co-protein, increases the yield of native folded LDH from 12 to 30% after 1000 s of folding when, in all cases, the reaction ceases to accelerate. They do not increase the rate of the folding process. The lagtime for LDH refolding alone is 380 s (Figure 11A), while this is increased to 570 s when folding is in the presence of cpn60 and ATP (Figure 11B), and when cpn10 is also present the lagtime reduces to 400 s (Figure 11C). The co-protein is not necessary for the increase in yield, but it does reduce the lagtime for folding over that seen with cpn60 alone.

DISCUSSION

The important in vitro property of chaperonins is their ability to increase the yield of the native form of a protein when refolding from denatured states (Goloubinoff et al., 1989; Buchner et al., 1991; Martin et al., 1991; Mendoza et al., 1991). This reflects their biological role in assisting the folding of newly synthesized proteins and proteins denatured as a result of cellular stress. To achieve this, the chaperonin must interact with misfolded structures and/or folding intermediates (van der Vies et al., 1992) and release them in a form which either folds more competently or is native. This binding/release cycle is coupled with, and driven by, the binding and hydrolysis of Mg–ATP and is assisted by the co-protein cpn10 (Goloubinoff et al., 1989; Ostermann et al., 1989; Buchner et al., 1991). In this paper, we have attempted to establish the nature and stability of interactions formed between cpn60, cpn10, and nucleotides and begin to map the complexes formed in the chaperonin hydrolytic cycle.

Conformational Changes in Cpn60. On the evidence that both Mg–ATP and Mg–AMP-PNP can displace bound protein, it has been suggested that the chaperonins exist in two forms, one which binds tightly to nonnative proteins but weakly to Mg–ATP and the other which binds Mg–ATP tightly and proteins weakly (Badcoe et al., 1991; Baneyx & Gatenby, 1992). This implies that the binding of the nucleoside triphosphate, rather than its hydrolysis, is responsible for the rearrangement which allows release of bound protein. The results presented here support this assertion.

It is known that apo-cpn60 is the form which binds most tightly to proteins and in the dye–protein conjugate the fluorescence of this species is low. The binding of either Mg–ATP or Mg–AMP-PNP weakens the interaction with substrate proteins, and in this state we see the same enhanced fluorescence in the conjugate. The binding of ATP occurs in two steps; an initial weak interaction with the apo-cpn60 conformation followed by a slow, cooperative rearrangement. During this rearrangement the binding affinity of Mg–ATP increases by a factor of at least 400. Thus binding is used to drive structural change. Potentially, the binding energy each subunit can contribute to the rearrangement is over 3 kcal/mol. We propose that this structural change is reponsible for shedding bound protein from the complex. This conclusion is supported by the weakened interaction of the ATP analogue when a peptide is bound to cpn60 (see Figure 8); thus, the nucleotide and peptide compete. Mg–AMP-PNP binds more weakly (as it does to many ATP-binding proteins), an

observation which explains its lower efficiency in displacing protein substrates (Schmidt & Buchner, 1992). The structural rearrangement of cpn60 driven by ATP and AMP-PNP has recently been visualized by electron microscopy (H. Saibil, S. Wood, and R. J. Ellis, personal communication) which reveals a gross change in subunit orientation within the oligomer.

We also show that Mg–ADP is able to bind weakly and cooperatively to cpn60. Moreover, cpn10 binds with very high affinity (K_d = 0.5–3 nM) to the cpn60 Mg–ADP complex. The formation of cpn10 complexes with cpn60/ADP has also been demonstrated by centrifugation (Bochkareva et al., 1992). Owing to the fact that, as yet, little is known about the behavior of complexes containing Mg–ADP and cpn10, either structurally or in their ability to bind nonnative proteins, we do not interpret the fluorescence changes which accompany these interactions as reflecting functional states. This is especially true in the case of the complex with cpn10, a large protein ligand rather than one which has a localized binding site. Despite the high stability of the cpn60/Mg–ADP/cpn10 complex (the $K_{1/2}$ for ADP binding is <70 nM) it is formed very slowly at low ADP concentrations and is likely to be produced in vivo by hydrolysis of a Mg–ATP state. Evidence for the formation of a stable cpn60/Mg–ADP/cpn10 complex by in situ hydrolysis of ATP has recently been produced by Bochkareva and co-workers (Bochkareva et al., 1992), and our results are in agreement with their proposed mechanism for formation of this ternary complex. Measurements of the protein stoichiometry of this state show that there are 14 subunits and only 7 of cpn10. This result equates with electron microscopy studies in which the cpn10 oligomeric single ring associates with only one side of the cpn60 double ring (Saibil et al., 1991; Ishii et al., 1992).

The co-protein, cpn10, enhances the binding of all nucleotides tested, so it will assist protein displacement as has been shown experimentally (Laminet et al., 1990; Buchner et al., 1991; Martin et al., 1991; Bochkareva et al., 1992). In addition, cooperativity of nucleotide binding is increased by the presence of cpn10, an observation also made in the experiments measuring the rate of ATP hydrolysis (Gray & Fersht, 1991). In the case of Mg–ATP binding, the Hill coefficient is 4 in the absence of cpn10 and 6 in its presence. This increased cooperativity will provide a more concerted structural rearrangement, so assisting the release of bound protein through a coordinated loss of affinity on all subunits, as exemplified in Figure 11.

Hydrolysis of ATP. The steady-state and "single-turnover" rates of ATP hydrolysis in cpn60 are both approximately 0.04 s^{-1} (see Figure 9A and 10), demonstrating that product release is not the rate-limiting step in the hydrolytic cycle. Cpn10 halves the rate of steady-state Mg–ATP turnover resulting from an inhibition of hydrolysis on only half of the cpn60 subunits, thus confirming the stoichiometry of cpn10 binding derived from fluorescence methods (see Figure 7). This functional "nonidentity" of the subunits in cpn60 when cpn10 is bound has also been deduced from Hill analysis of ATP binding data (Bochkareva et al., 1992).

Not only is cpn10 able to inhibit hydrolysis of Mg–ATP, but it also forms a very stable complex with cpn60 and ADP (Figure 5B); i.e., it reduces the rate of ADP release. These observations show the cpn60/cpn10 complex to be stable irrespective of the state of the nucleotide ligand (Bochkareva et al., 1992). They are also in accord with cpn10 halving the Mg–ATP consumption by remaining part of the complex through several cycles of fast hydrolysis when stimulated by the binding of unfolded protein (Figure 9B).

Chaperonin Assisted Refolding of Lactate Dehydrogenase. The contribution of cpn10 to chaperonin-mediated folding depends on the protein substrate. In the case of rhodanese, it is necessary for release of the protein from the complex (Martin et al., 1991); for dihydrofolate reductase (Martin et al., 1991), and pre-β-lactamase (Laminet et al., 1990) it greatly accelerates this process and for citrate synthase it augments the yield of active enzyme (Buchner et al., 1991). The effect on bacterial LDH used here is to hasten the appearance of native protein, although it does not significantly improve the yield over that seen with just cpn60 and ATP. Thus, in all cases cpn10 stimulates protein release but the magnitude of the effect is variable. It is possible that proteins which have a high affinity for cpn60 and/or a small free energy of folding are those which rely most heavily on the co-protein.

The more important conclusion to be drawn from the results shown in Figure 11 is that they contradict the idea that chaperonins work purely by lowering the concentration of unfolded protein molecules in order to suppress aggregation. As described in the introduction, this mechanism will lead to a reduction in the folding rate concomitant with increased yield. When cpn60, ATP, and cpn10 are included in the refolding medium, the rate of folding over that seen for LDH alone is essentially the same, but the yield is increased 2–3-fold.

Catalytic Cycle. A good basis for understanding the process of energy transduction in chaperonins is provided by defining the molecular events in the cycle of Mg–ATP binding, hydrolysis, and product release. For the purpose of this discussion, the two conformers of cpn60 are designated cpn60-(P) for the apo structure which interacts tightly with unfolded protein substrate and cpn60(A) for the structure which interacts tightly with ATP and weakly with substrate proteins. In the absence of cpn10 and beginning with cpn60(P) the events are as follows.

(A) Mg–ATP forms a weak collision complex with cpn60-(P). In this step, binding is noncooperative with a dissociation constant of 4 mM and generates cpn60(P)/ATP.

(B) This complex then undergoes a cooperative structural rearrangement with a rate constant of 180 s^{-1} which increases its affinity for Mg–ATP by at least 400-fold. This rearrangement is responsible for the loss of affinity for unfolded proteins. This new state is cpn60(A)/ATP.

(C) The rearranged cpn60(A) hydrolyzes Mg–ATP at a rate of 0.038 s^{-1}.

(D) The products are weakly bound and dissociate rapidly and the chaperonin returns to its original structure cpn60(P) which has a high affinity for unfolded proteins.

When an unfolded protein binds to the cpn60(A) state, the rate of hydrolysis is increased markedly so, producing the cpn60(P) state which interacts with the substrate protein more tightly. Thus, Mg–ATP hydrolysis on the complex, far from stimulating the release of bound protein, tightens its interaction with the chaperonin. Reassociation of Mg–ATP then drives cpn60 into the cpn60(A) state, thus weakening the interaction with the substrate protein.

The results presented in Figure 11 show that cpn60 and Mg–ATP can improve folding efficiency even when cpn10 is absent, an observation also made by others (Laminet et al., 1990; Buchner et al., 1991). This is the simplest system which is able to direct the energy of Mg–ATP hydrolysis into the folding process. The results presented in this paper show that the role of Mg–ATP binding and turnover is to cycle the chaperonin between a state which interacts weakly with the protein substrate and one which interacts tightly.

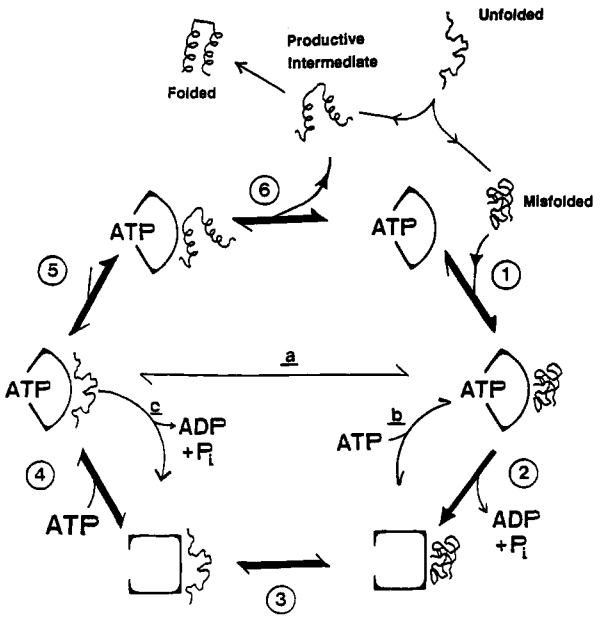

FIGURE 12: Hypothetical scheme for the action of chaperonins in assisting protein folding. This mechanism is intended to explain our results in the absence of cpn10. Steps in the productive cycle for assisting folding are numbered 1–6. (step 1) Misfolded protein binds weakly to the surface of cpn60(A)/ATP. (step 2) The protein–protein interaction stimulates ATP hydrolysis; ADP and P_i are released. (step 3) The chaperonin is now converted to the form that binds unfolded proteins tightly, i.e., cpn60(P). The misfolded substrate is driven into a less folded form. (step 4) Reassociation of ATP returns the chaperonin to its cpn60(A)/ATP state. (step 5) Having lost affinity for the chaperonin, the bound protein can then form intramolecular contacts. (step 6) The more productive, native-like species is bound very weakly and dissociates rapidly. Epicycles are produced by step a, spontaneous misfolding, while bound to the chaperonin; step b continued hydrolysis of ATP with the substrate in the misfolded state; and step c continued hydrolysis of ATP with the substrate in the unfolded form. These epicycles explain the high stoichiometry of ATP consumption per protein molecule folded and for the differences between protein substrates.

Hypothesis for Chaperonin Function. The question arises as to how this ATP-driven cycle in cpn60 is able to increase protein folding efficiency. One hypothesis which may account for our observations is summarized in Figure 12 and described below.

Protein folding from the random coil state in vitro begins with a very rapid collapse of the protein chain (Kim & Baldwin, 1990). This process may generate a range of intermediate species (Radford et al., 1992), with varying amounts of localised native-like structure and nonnative exposed hydrophobic surface. This may include unproductive misfolded conformations, as well as productive folding intermediates. The unproductive structures must rearrange to a productive state in order to fold correctly. If this rearrangement is slow, these poorly folded states are arrested and may aggregate. Previous work shows that cpn60 binds to unfolded proteins via hydrophobic interactions (Tandon & Horowitz, 1986; Mendoza et al., 1991; Landry et al., 1992) and so will selectively bind those structures with the greatest exposure of nonpolar residues. It is the distribution between productive and nonproductive collapsed intermediates which may dictate the folding efficiency of the protein. When this mixed population is introduced to a cpn60/Mg–ATP solution, it will first encounter the steady-state complex, cpn60(A)/ATP. The least native-like bind tightest (Figure 12, step 1) owing to their greater surface hydrophobicity and trigger hydrolysis of Mg–ATP (Figure 12, step 2). This converts the chaperonin to the cpn60(P) structure which binds the poorly folded protein substrate more even more tightly. The substrate is then driven into a less folded state because the exposed hydrophobic area with which the chaperonin can interact is then increased (Figure 12, step 3). This ability of cpn60(P) (i.e., the apo form) to drive proteins into more unfolded states has been observed in studies with pre-β-lactamase and dihydrofolate reductase as the substrates (Laminet et al., 1990; Viitanen et al., 1990). In addition, with bacterial lactate dehydrogenase, cpn60 arrests folding only when folding is initiated from the random coil state rather than from a partially unfolded "molten globule"-like conformation (Badcoe et al., 1991; Smith et al., 1991). Rebinding Mg–ATP (Figure 12, step 4) weakens the protein–chaperonin interaction, allowing the substrate to rearrange and form intra- rather than intermolecular hydrophobic contacts (Figure 12, step 5). If the new, spontaneously formed conformation is poorly folded, then Mg–ATP will again be hydrolyzed. This process will cycle until the protein substrate acquires a more native-like conformation with reduced hydrophobic surface. Such structures will be released (Figure 12, step 6) and are able to fold more productively. In this mechanism, cpn60 performs two tasks. First, it lowers the energy barrier between misfolded states and either the native state or, more probably, a productive intermediate, by stabilizing more unfolded "transition" states. Such activities for molecular chaperones have been suggested before (Hubbard & Sandor, 1991; Weissman & Kim, 1991). Second, it sequesters the folding protein on the chaperonin until it acquires a native-like conformation.

The former effect can be likened to that of a selective and reversible protein denaturant. If a protein folds with only 50% efficiency from its denatured state and the 50% which has misfolded could be selected, denatured, and allowed to refold, then a further 25% of the original sample would fold correctly. Repetition of this process of selective denaturation followed by renaturation will result in a very high folding yield. In this analogy, the energy derived from ATP binding and hydrolysis is used to cycle the chaperonin between a selective binder (cpn60(A)/ATP) and a denaturant (cpn60-(P)). Such a crude mechanism would account for the lack of substrate specificity of chaperonins.

ACKNOWLEDGMENT

We thank Dr. W. Mawby for supplying the peptide used in our experiments, Dr. H. Saibil for access to data on structural rearrangements in chaperonins, and Drs. P. Lund and S. Halford for general discussion of results. We would particularly like to thank Mrs. G. Salt for keeping the Bristol laboratory in running order. G.S.J. acknowledges a studentship from the SERC (U.K.), and R.A.S. acknowledges personal support from Porton Industries, Salisbury, U.K. The stopped-flow and equilibrium experiments described in this paper were carried out on apparatus paid for by the Protein Engineering Initiative of the SERC (U.K.). A.R.C. and S.G.B. thank the Wellcome Trust for the award of a grant to fund this work.

REFERENCES

Ames, B. N. (1966) *Methods Enzymol. 8*, 115–118.

Badcoe, I. G., Smith, C. J., Halsall, D. J., Holbrook, J. J., Lund, P., & Clarke, A. R. (1991) *Biochemistry 30*, 9195–9200.

Baneyx, F., & Gatenby, A. A. (1992) *J. Biol. Chem. 267*, 11637–11644.

Bochkareva, E. S., Lissin, N. M., Flynn, G. C., Rothman, J. E., & Girshovich, A. S. (1992) *J. Biol. Chem. 267*, 6796–6800.

Brown, K. L., Wood, S., & Buttner, M. J. (1992) *Mol. Microbiol. 6*, 1133–1140.
Buchner, J., Schmidt, M., Fuchs, M., Jaenicke, R., Rudolph, R., Schmid, F.-X., & Kiefhaber, T. (1991) *Biochemistry 30*, 1586–1591.
Chandrasekhar, G. N., Tilley, K., Woolford, C., Hendrix, R., & Georgopoulos, C. (1986) *J. Biol. Chem. 261*, 12414–12419.
Clarke, A. R., Waldman, A. D. B., Munro, I., & Holbrook, J. J. (1985) *Biochim. Biophys. Acta 828*, 375–379.
Ellis, R. J., & van der Vies, S. M. (1991) *Annu. Rev. Biochem. 60*, 321–347.
Gatenby, A. A., & Ellis, R. J. (1990) *Annu. Rev. Cell Biol. 6*, 125–149.
Gething, M.-J., & Sambrook, J. (1992) *Nature 355*, 33–45.
Godchaux, W., & Zimmerman, W. F. (1979) *J. Biol. Chem. 254*, 7874–7884.
Goloubinoff, P., Christeller, J. T., Gatenby, A. A., & Lorimer, G. H. (1989) *Nature 342*, 884–889.
Gray, T. E., & Fersht, A. R. (1991) *FEBS Lett. 292*, 254–258.
Hendrix, R. (1979) *J. Mol. Biol. 129*, 375–392.
Hohn, T., Hohn, B., Engel, A., Wurtz, M., & Smith, P. R. (1979) *J. Mol. Biol. 129*, 359–373.
Hubbard, T. J. P., & Sander, C. (1991) *Protein Eng. 4*, 711–717.
Ishii, N., Tagushi, H., Sumi, M., & Yoshida, M. (1992) *FEBS Lett. 299*, 169–174.
Jenkins, A. J., March, J. B., Oliver, I. R., & Masters, M. (1986) *Mol. Gen. Genet. 202*, 446–454.
Kim, P. S., & Baldwin, R. L. (1990) *Annu. Rev. Biochem. 59*, 631–660.
Kouyami, T., & Mihashi, K. (1981) *Eur. J. Biochem. 144*, 33–38.
Laminet, A. A., Ziegelhoffer, T., Georgopoulos, C., & Pluckthun, A. (1990) *EMBO J. 9*, 2315–2319.
Landry, S. J., Jordan, R., McMacken, R., & Gierasch, L. M. (1992) *Nature 355*, 455–457.
Leatherbarrow, R. J. (1990) Grafit v.2.0. Erithracus Software Ltd, Staines, U.K.
Lorimer, G. H. (1992) *Curr. Opin. Struct. Biol. 2*, 26–34.
Marquardt, D. W. (1963) *J. Soc. Ind. Appl. Math 11*, 431–441.
Martin, J., Langer, T., Boteva, R., Schramel, A., Horwich, A. L., & Hartl, F.-U. (1991) *Nature 352*, 36–42.
Mendoza, J. A., Rogers, E., Lorimer, G. H., & Horowitz, P. M. (1991) *J. Biol. Chem. 266*, 13044–13049.
Ostermann, J., Horwich, A. L., Neupert, W., & Hartl, F.-U. (1989) *Nature 341*, 125–130.
Radford, S. E., Dobson, C. M., & Evans, P. A. (1992) *Nature 358*, 302–307.
Rothman, J. E. (1989) *Cell 59*, 591–601.
Saibil, H., Dong, Z., Wood, S., & auf der Mauer, A. (1991) *Nature 353*, 25–26.
Schmidt, M., & Buchner, J. (1992) *J. Biol. Chem. 267*, 16829–16833.
Sherman, M. Y., & Goldberg, A. L. (1992) *Nature 357*, 167–169.
Smith, C. J., Clarke, A. R., Chia, W. N., Irons, L. I., Atkinson, T., & Holbrook, J. J. (1991) *Biochemistry 30*, 1028–1036.
Tandon, S., & Horowitz, D. (1986) *J. Biol. Chem. 261*, 15615–15618.
van der Vies, S. M., Viitanen, P. V., Gatenby, A. A., Lorimer, G. H., & Jaenicke, R. (1992) *Biochemistry 31*, 3635–3644.
Viitanen, P. V., Donaldson, G. K., Lorimer, G. H., Lubben, T. H., & Gatenby, A. A. (1991) *Biochemistry 30*, 9716–9723.
Weismann, J. S., & Kim, P. S. (1991) *Science 253*, 1386–1393.
Zeilstra-Ryalls, J., Fayet, O., & Georgopoulos, C. (1991) *Annu. Rev. Microbiol. 45*, 301–325.
Zimmerman, S. B. (1963) *Methods Enzymol. 6*, 258–262.